ELSEVIER

Journal of Photochemistry and Photobiology A: Chemistry 108 (1997) 197–205

Journal of PHOTOCHEMISTRY AND PHOTOBIOLOGY A: CHEMISTRY

Fate of amino acids upon exposure to aqueous titania irradiated with UV-A and UV-B radiation Photocatalyzed formation of NH_3, NO_3^-, and CO_2

H. Hidaka [a,*], S. Horikoshi [a], K. Ajisaka [a], J. Zhao [a,1], N. Serpone [b]

[a] *Department of Chemistry, Meisei University, 2-1-1, Hodokubo, Hino, Tokyo 191, Japan*

[b] *Laboratory of Pure and Applied Studies in Catalysis, Environment and Materials, Department of Chemistry and Biochemistry, Concordia University, 1455 deMaisonneuve Blvd. West, Montreal, Quebec, Canada H3G 1M8*

Received 11 December 1996; accepted 17 February 1997

Abstract

The fate of nitrogen in various amino acids was examined following their photooxidative (and/or reductive) transformation catalyzed by UV-A and UV-B illuminated aqueous TiO_2 dispersions. The nitrogens in the amino acids are photoconverted predominantly into NH_3 (analyzed as NH_4^+) and to a lesser extent into NO_3^- ions; NH_4^+/NO_3^- ratios span the range 3–12 after ca. 8 h irradiation. Extensive evolution of CO_2 is also observed; in some cases it is quantitative. Variations in the NH_4^+/NO_3^- ratio in the transformation of amino acids are dependent on the substrates molecular structure. Some of the steps in an otherwise complex mechanism of the heterogeneous photocatalyzed mineralization are described. © 1997 Elsevier Science S.A.

Keywords: Photodegradation; Photooxidation; Photocatalysis; Titanium dioxide; Amino acid

1. Introduction

Recent studies on the TiO_2-catalyzed photodegradation of a variety of nitrogen-containing organics have focused attention on the purification and treatment of water and air [1–5]. In particular, such herbicides and pesticides as benzamide [1], pyridine [2], atrazine [3], and s-triazines [4] having nitrogen(s) in their skeleton have been examined. Hazardous nitrogen-containing aromatics [5] and gas generating reagents [6] were also investigated. We and others have extensively examined a large variety of nitrogen-containing surfactants [7,8]. The decarboxylation and deamination of several amino acids by attack by •OH radicals in homogeneous aqueous media has been reported by Monig et al. [9] who also provided mechanistic implications in some detail. Biochemical applications of TiO_2-mediated photooxidations are promising for the elimination of microorganisms, e.g. bacteria, fungi, mold, and virus, among others. In vivo suppression of cancer cells by illuminated titania systems was recently reported by Fujishima and coworkers [10]. However, simpler systems of biochemical interest have not been the subject of systematic studies to assess the fate of the elemental constituents of such systems. Of particular importance are the amino acids which are the building blocks of proteins.

Studies of the reactions of various amino acids with •OH radicals and solvated electrons, e_{aq}^-, produced in pulsed and CW radiolysis experiments [9,11–16] have provided several salient mechanistic features regarding the modes of attack by these radicals in homogeneous aqueous media.

In this paper we describe the photocatalyzed transformation of a series of amino acids of different structures, and report on the formation of NH_4^+ and NO_3^- ions originating from photooxidative (and/or reductive) processes during their mineralization in aqueous titania dispersions illuminated with UV-A and UV-B radiation (400–320 nm and 320–290 nm, respectively). Attention is also focused on cleavage of the peptide bond during the phototransformation of amino functions to ammonium and nitrate ions.

2. Experimental section

The amino acids shown in their zwitterionic forms (Table 1) examined in this study under near-neutral condi-

* Corresponding author.

[1] Present address: Institute of Photographic Chemistry, Chinese Academy of Sciences, Beisatan, Beijing 10010, China.

PII S1010-6030(97)00089-0

Table 1
List of amino acids and related compounds examined in this study

No.	Name	Abbreviated name	Structure
	Amino Acids		
1.	L-α-Alanine	α-Ala	CH_3-CH(NH_3^+)-COO^-
2.	β-Alanine	β-Ala	^+H_3N-CH_2-CH_2-COO^-
3.	L-Valine	Val	$(CH_3)_2$-CH-CH(NH_3^+)-COO^-
4.	L-Leucine	Leu	$(CH_3)_2$-CH-CH_2-CH(NH_3^+)-COO^-
5.	L-iso-Leucine	Ile	CH_3-CH_2-CH(CH_3)-CH(NH_3^+)-COO^-
6.	L-Serine	Ser	$HOCH_2$-CH(NH_3^+)-COO^-
7.	L-Threonine	Thr	CH_3-CH(OH)-CH(NH_3^+)-COO^-
8.	L-Aspartic Acid	Asp	^-OOC-CH_2-CH(NH_3^+)-COO^-
9.	L-Glutamic Acid	Glu	^-OOC-CH_2-CH_2-CH(NH_3^+)-COO^-
10.	L-Glutamine	Gln	H_2N-C(=O)-CH_2-CH_2-CH(NH_3^+)-COO^-
11.	L-Cysteine	Cys	HS-CH_2-CH(NH_3^+)-COO^-
12.	L-Methionine	Met	CH_3-S-CH_2-CH_2-CH(NH_3^+)-COO^-
13.	L-Phenylalanine	Phe	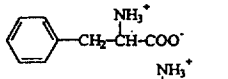
14.	L-Tryptophan	Trp	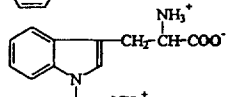
15.	L-Histidine	His	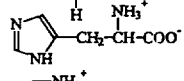
16.	L-Proline	Pro	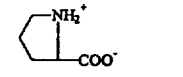
17.	L-Arginine	Arg	$^+H_3NCNH$-$(CH_2)_3$-CH(NH_3^+)-COO^-
	Ester of a Dipeptide		
Aspartame		Methyl ester of Phe-Asp	^+H_3N-CH($CH_2C_6H_5$)-C(=O)-NH-CH(^-OOC-CH_2)-C(=O)-OCH_3
	Miscellaneous		
N-Dodecanoylglutamate		C_{12}-L-Glu	$CH_3(CH_2)_{10}$-C(=O)-NH-CH(COO^-)-CH_2CH_2-COO^-
N-Dodecanoyl-β-Alanine		C_{12}-β-Ala	$CH_3(CH_2)_{10}$-C(=O)-NH-CH(COO^-)-CH_3

tions (pH 6–7) were all supplied by Tokyo Kasei Co. Ltd.; aspartame (the methyl ester of Phe-Asp), sodium *N*-dodecanoyl glutamate (C_{12}-L-Glu) and *N*-dodecanoyl-β-alanine (C_{12}-β-Ala) were kindly provided by Ajinomoto Co. Ltd. The TiO_2 (P-25) photocatalyst, supplied by Degussa AG, was mostly anatase particles (ca. 80%) with a surface area of 55 $m^2\ g^{-1}$. Deionized and doubly distilled water was used throughout (pH of water was 6.3).

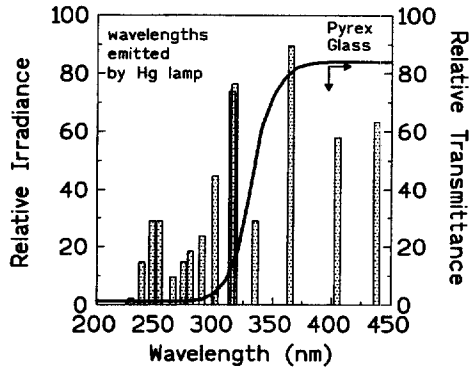

Fig. 1. Graph illustrating the wavelengths emitted by the Hg lamp and a profile of the light transmittance by the pyrex reactor used. The UV-A (400–320 nm) and UV-B (320–290 nm) wavelengths were used to excite the TiO_2 photocatalyst particles which absorb radiation at wavelengths below 387 nm (bandgap energy of TiO_2 anatase, 3.2 eV).

Oxygen-saturated aqueous solutions of each amino acid (0.1 mM; 50 ml) containing TiO_2 (100 mg) were irradiated with a 75 W Hg-lamp (Fig. 1; Toshiba SHLS-1002A lamp; in the wavelength region of interest, 310–400 nm, energy emitted was 2.46 mW cm^{-2} at 10 cm from lamp). Ammonium ions were analyzed with a JASCO ion chromatograph equipped with a CD-5 conductivity detector using a Y-521 cationic column with a HNO_3 solution (4 mM) as the eluent. Nitrate ions were monitored by ion chromatography with an I-524 anionic column using a mixed eluent of phthalic acid (2.5 mM) and tris(hydroxymethyl)aminomethane (2.3 mM); the pH was adjusted to 4.0. The temporal evolution of carbon dioxide from the photodegradation was assayed using an Ohkura gas chromatograph (Model 802) fitted with a Porapak Q column and a thermal conductivity detector. The peroxide value (POV) of the photodegraded aqueous mixture (0.1 ml aliquots; 50 ml solutions; 100 mg TiO_2) was measured in an iso-octane–acetic acid (ratio 1:4) solvent mixture using the potassium iodide procedure [17].

3. Results and discussion

Reaction of e^- with simple aliphatic α-amino acids leads to deamination (Eq. (1))

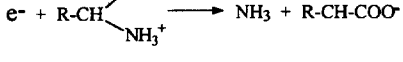

(1)

in competition with H• atom formation (Eq. (2)) [9]:

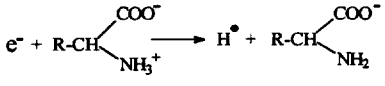

(2)

In principle, •OH radicals can abstract H atoms from anywhere in the aliphatic chain. However, to the extent that the protonated amino function, $-NH_3^+$, deactivates the α-C–H bond, it directs this electrophilic attack by •OH radicals at C–H bonds located further away from the α-carbon (Eq. (3)):

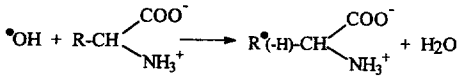

(3)

If the amino function is unprotonated, then the •OH radical attacks the α-carbon preferentially (Eq. (4)) [11]:

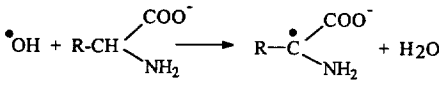

(4)

The principal products of reactions (1)–(3) are NH_3, R–COOH and keto-acids, with only minor evolution of CO_2, the extent of which was considered unimportant.

By contrast, very effective decarboxylation of α-amino acids by •O:H radicals takes place in alkaline aqueous solutions under conditions where the amino function is unprotonated; the •OH radical attacks the free electron pair of the nitrogen atom (Eq. (5)) [9]:

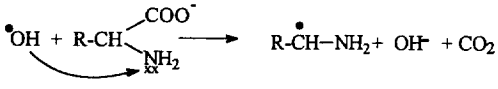

(5)

A prerequisite for the reactions is that both the $-NH_2$ and –COOH functions be on the same carbon atom. Where these functions are on different carbon atoms, very little CO_2 is evolved irrespective of pH; for example, the CO_2 yield from β-Ala (expressed as the G yield) was ca. 0.4 at pH 9.1; the G yield of CO_2 formation from α-Ala was 4.4 to 5.3 in the pH range 9.0 to 11.9 [9]. Reaction with •OH radicals yields CO_2 only if the amino function in α-Ala is unprotonated (Eqs. (6a) and (6b)):

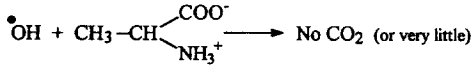

(6a)

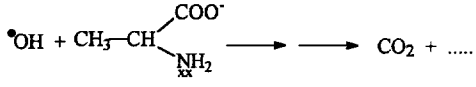

(6b)

In acid/neutral aqueous media in which the amino function is fully protonated, H-atom abstraction occurs from C–H bonds remote from the carbon carrying the $-NH_2$ and $-COO^-$ groups.

Attack of •OH radicals at the $-NH_2$ function competes with H-atom abstraction from anywhere in the carbon skeleton of the amino acids for which CO_2 evolution is unimportant in homogeneous media; [9] the relative rates are dependent on (i) the type of C–H bonds, (ii) the degree of C–H bond activation by the neighboring groups, and to a significant extent on (iii) the structure of the amino acids. The rate of abstraction of a hydrogen in position α to $-NH_2$ and $-COO^-$ groups (see Eqs. (6a) and (6b)) is about five times greater than analogous rates for abstraction of either a β-hydrogen or a γ-hydrogen. As well, an increasing number of C–H bonds results in an increasing probability of H-atom abstraction and consequently leads to lower yields of carbon dioxide from elimination of the $-COO^-$ moiety.

Three different structural effects influence [9] the extent of CO_2 evolution: (i) the carbon skeleton (R–CH) of the amino acids is an aliphatic chain, (ii) the R group in the amino acid contains an OH substituent in the skeleton (e.g., threonine; Table 1), and (iii) the structural variations in the aliphatic chain of the amino acids, e.g. $(CH_3)_2C(NH_2)$-COO^- vs. $CH_3CH_2CH(NH_2)COO^-$ for which a greater CO_2 yield is obtained in the former. As an example of structural effects in the alkyl chain, the G yield of carbon dioxide from the decarboxylation of leucine is greater than the yield from *iso*-leucine (4.2 vs. 3.2 at pH 11.9) [9].

No nitrate ion formation was ever found in these earlier studies, at least none was reported [9,11–16].

3.1. Heterogeneous photocatalyzed conversion of amino acids

The temporal evolution of ammonium and nitrate ions produced by the TiO_2-photocatalyzed mineralization of α-Ala and β-Ala is illustrated in Fig. 2(a). After a small ($\approx$ 10 min) induction period, near-quantitative (96%) conversion of the $-NH_2$ nitrogen into NH_4^+ ion from α-Ala occurs (Table 2) via a first-order process slightly faster than for the β-Ala analog; the latter shows 87% conversion to ammonium ions after an 8 h irradiation period (Table 3). By contrast, β-Ala produces a greater yield of NO_3^- ions (7%) than does α-Ala ($\approx$2%). Mineralization of α-Ala to CO_2 takes place quantitatively and concomitantly with ammonium ion formation at nearly identical rates (Table 2); CO_2 evolution (81% yield after 8 h illumination) from β-Ala is three-fold faster. No induction period is evident in formation of carbon dioxide (Fig. 2(b)). During the degradation process, peroxide intermediates (Fig. 2(c)) formed and were subsequently degraded; they are produced in greater yield in α-Ala than in the β-analog.

The first-order rates of formation of ammonium and nitrate ions, together with the kinetic evolution of carbon dioxide from other α-amino acids (Val, Leu and Ile) with alkyl chains are summarized in Table 2; the corresponding yields of CO_2 after an 8 h illumination period are presented in Table 3. The rates of formation of NH_4^+, NO_3^- and CO_2 increase in the order, respectively, α-Ala $\approx$ Val $\approx$ Leu < Ile; Val $\approx$ Leu < Ile; and Ile < Leu < α-Ala < Val. The corresponding yields of the mineralization products vary in the order, for NH_4^+ ions: α-Ala (96%) > Val (77%) > Leu (73%) > Ile (67%); for NO_3^- ions: Leu (18%) $\approx$ Ile (18%) > Val (10%) > α-Ala ($\approx$2%); and for CO_2: α-Ala (100%) $\approx$ Leu (100%) > Ile (86%) > Val (69%). Contrary to earlier findings in homogeneous aqueous media [9], these yields do not scale with

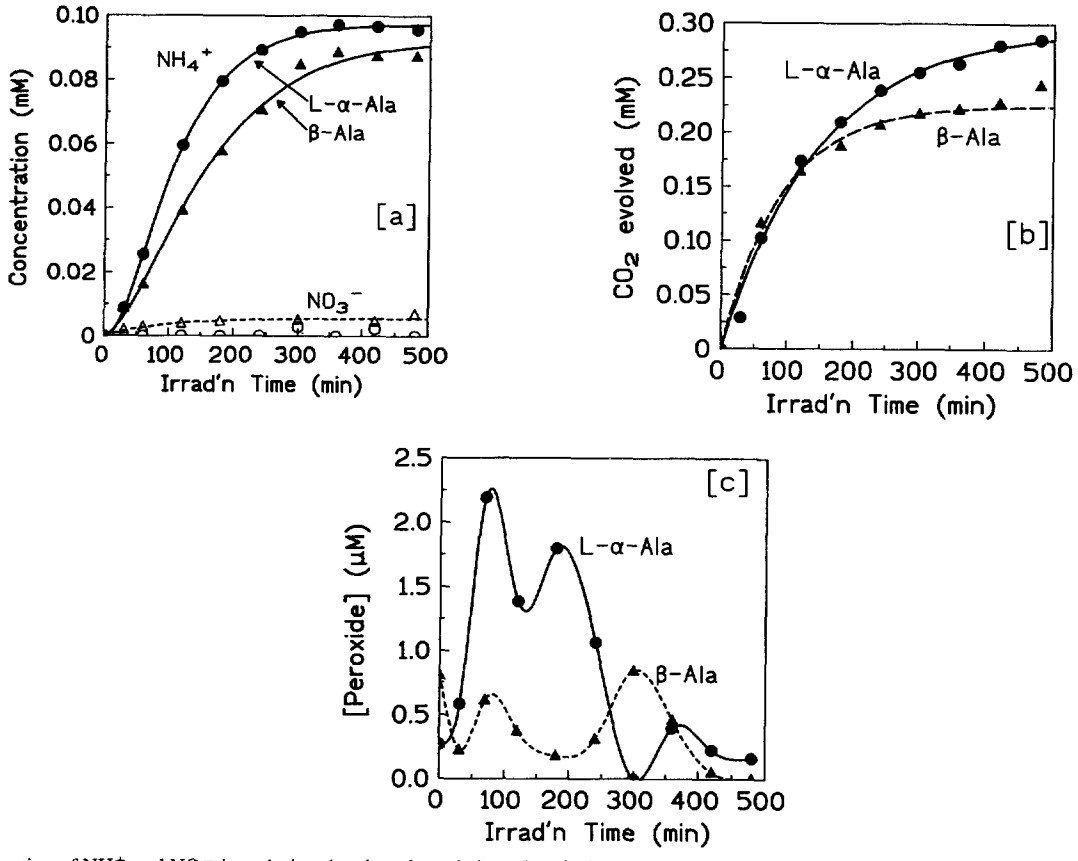

Fig. 2. (a) Formation of NH_4^+ and NO_3^- ions during the photodegradation of α-alanine and β-alanine (0.1 mM) in oxygen-saturated aqueous suspensions of TiO_2 (100 mg; 50 ml solutions) under Hg-lamp illumination. (b) CO_2 evolution under the same conditions as in (a). (c) Formation and degradation of peroxide species resulting from the degradation of α- and β-alanine under the same conditions as in (a).

the number of C–H bonds. Evidently, other factors must influence both the yields and the rates of formation of NH_4^+, NO_3^-, and CO_2 in heterogeneous media. In addition to the factors implied above, the surface of the photocatalyst TiO_2 and its interactions with each of the amino acids must (no doubt) play an important role.

Serine and threonine also are α-amino acids with the alkyl chain containing an OH substituent in the β-carbon, albeit with different number of carbons and C–H bonds. As in the alkylated α-amino acids, the amino function is photocatalytically converted predominantly to NH_4^+ ions rather than NO_3^- ions (ratio ≈ 8 for Ser and ≈ 3 for Thr for 8 h illumination; Table 2) at rates about two-fold faster than the alkylated analogs. Evolution of carbon dioxide is quantitative (100%) for Ser; it is 76% for Thr for the same period of irradiation, in accord with the number of C–H bonds (3 for Ser versus 5 for Thr; Table 1).

Aspartic acid (Asp) and glutamic acid (Glu) are both α-amino dicarboxylic acids and contain three and five C–H bonds, respectively. Though the nitrogen is quantitatively converted into NH_4^+ and NO_3^- ions overall (see Fig. 3 below; ratios: 9.6 and 8.2, respectively; Table 2) the yields of CO_2 after 8 h are 61% (Asp) and 78% (Glu) and do not accord with the number of C–H bonds present. Clearly, the presence of groups on the alkyl chain in these α-amino acids does not permit a direct relationship between the quantity of CO_2 formed and the number of C–H bonds, which earlier was shown [9] to be expected if decarboxylation of the amino acid $-COO^-$ function was the sole source of CO_2. In the present work, carbon dioxide evolution implicates all carbon atoms.

The temporal evolutions of ammonium and nitrate ions in glutamine (Gln), glutamic acid (Glu) and *N*-dodecanoylglutamic acid, C_{12}-Glu, are depicted in Fig. 3. After 8 h illumination, the quantity of NH_4^+ ions varies as Gln > Glu > C_{12}-Glu with the quantity of NO_3^- ions about equal for these three amino acids (about 10–13%). This suggests that NO_3^- ions are generated from the photooxidation of the α-NH_2 function, and not from the $-NH_2$ of the amide group in glutamine. The NH_4^+/NO_3^- ratios (Table 2) vary in the order Glu (8.2) > Gln (7.5) > C_{12}-Glu (6.2) illustrating the effect the structure of the amino acid has on the evolution of ammonium versus nitrate ions.

The temporal formation of NH_4^+, NO_3^- and SO_4^{2-} ions in the photomineralization of cysteine (Cys) and methionine (Met) are summarized in Figs. 4(a) and 4(b), respectively. Cysteine shows prompt evolution of the three ions, respectively, at rates 0.014 min^{-1}, 0.027 min^{-1} and 0.0095 min^{-1}, albeit the quantity of NH_4^+ ions formed is ca. 11 times greater than NO_3^- ions and the yield of SO_4^{2-} ions is ca. 63%. By

Table 2
Formation ratios of NH_4^+/NO_3^- and rate constants of formation of NH_4^+ and NO_3^- ions, and evolution of CO_2 in the photooxidative degradation of various amino acids [a] in aqueous titania suspensions

Compound	Ratio [b]		Rate constant ($\times 10^{-3}$ min^{-1})		
	2 h	8 h	NH_4^+	NO_3^-	CO_2
Amino acids					
1. L-α-Alanine	–	–	6.8±1.1	–	6.7±0.8
2. β-Alanine	9.3	12	4.2±0.8	9.8±2.3	11.8±1.4
3. L-Valine [c]	9.2	7.8	6.7±0.3	5.0±1.6	11.9±0.7
4. L-Leucine [c]	4.8	4.2	7.4±0.6	5.9±1.4	4.3±0.4
5. L-iso-Leucine [c]	5.9	3.8	20.0±0.5	9.0±1.4	3.8±0.3
6. L-Serine	9.0	7.9	16.6±1.0	16±5	15.3±1.0
7. L-Threonine [c]	6.9	3.1	24.3±3.5	1.0±0.6	25±3
8. L-Aspartic Acid	9.5	9.6	19.2±1.3	19.7±3.7	52±12
9. L-Glutamic Acid	8.1	8.2	20.5±2.7	13.4±2.4	24±4
10. L-Glutamine	47	7.5	7.2±0.4	1.2±0.7	11.4±1.2
11. L-Cysteine [d]	9.0	10.7	14.1±1.5	27±5	–
12. L-methionine [c,e]	12	10	11.3±0.6	5.3±1.2	10.5±0.6
13. L-Phenylalanine [c,f]	3.3	5.0	21.3±1.7	12.6±2.6	7.0±1.0
14. L-Tryptophan [c,g]	5.9	4.7	5.8±0.7	7.4±2.1 [h]	5.3±0.9
15. L-Histidine [c]	11	4.9	17.6±2.5	1.9±0.5	12.6±1.1
16. L-Proline	107	3.5	7.1±1.2	18±5 [h]	–
17. L-Arginine [c]	–	3.0	9.2±1.4	1.1±0.2 [i]	13.3±1.2
Miscellaneous related compounds					
Aspartame	–	9.8	8.1±0.7	10±3 [i]	–
C_{12}-L-Glutamate	11	6.2	5.4±0.2	2.4±1.0	–
C_{12}-β-Alanine	8.1	7.6	1.3±0.8	3.1±0.8	–

[a] The pK_{a1} for the –COOH group lies in the range 1.8–2.4; the pK_{a2} for the ammonium ion lies in the range 8.8–10.6 for amino acids with neutral side chains [18].
[b] Ratio at two different irradiation times.
[c] Essential amino acids that must be present in the diet of mammals to ensure normal growth.
[d] Rate of formation of SO_4^{2-} ions, $k = 9.5 \pm 0.7 \times 10^{-3}$ min^{-1}.
[e] Rateof formation of SO_4^{2-} ions: $k_{slow} = 2.1 \pm 0.2 \times 10^{-5}$ min^{-1} and $k_{fast} = 5.1 \pm 0.1 \times 10^{-3}$ min^{-1}.
[f] Rate of disappearance of phenylalanine, $k = 19 \pm 1 \times 10^{-3}$ min^{-1}.
[g] Rate of disappearance of tryptophan, $k = 27 \pm 4 \times 10^{-3}$ min^{-1}.
[h] After 1 h induction period.
[i] After 2 h induction period.

contrast, although conversion of nitrogen in methionine to NH_4^+ and NO_3^- ions is prompt with ammonium ions formed two-fold faster and in yields about an order of magnitude greater (Table 2), evolution of sulfate ions proceeds by a slow and a fast pathway, the latter occurring after ca. 5 h irradiation before significant quantities of SO_4^{2-} are produced (ca. 62% after an 8 h illumination period). Evidently, the thioether sulfur group in methionine is protected from being rapidly oxidized by the •OH radicals produced from illuminated TiO_2 (see below).

The α-amino acids phenylalanine (Phe) and tryptophan (Trp) both possess a β-CH_2 group and an aromatic ring(s). The loss of aromaticity through the fracture of the phenyl ring in Phe, monitored by UV absorption at 210 nm, necessitates 5 h of irradiation of the aqueous TiO_2 suspension, where as Trp loss of aromaticity is 95% complete after 2 h (Fig. 5(a)); there is a residual absorption at short wavelengths (around 218 nm) in the UV region up to 8 h of illumination, likely due to some intermediate species. The rate of decomposition of Phe, as determined by loss of UV absorption, is about three-fold faster (0.019 min^{-1}) than carbon dioxide evolution (0.007 min^{-1}) but occurs nearly concomitantly with formation of NH_4^+ ions after a small, ca. 10–20 min, induction period (0.021 min^{-1}; Table 2 and Fig. 5(b)); formation of NO_3^- ions also lags behind (0.013 min^{-1}). After an 8 h period, Phe is 62% mineralized (yield of CO_2). By contrast, degradation of Trp takes place about three-to-four times faster (0.027 min^{-1}) than production of either NH_4^+ or NO_3^- ions (0.0058 min^{-1} and 0.0074 min^{-1}, respectively) or CO_2 evolution (0.0053 min^{-1}). •OH radical attack probably occurs on the aromatic ring(s) before attack at the α-CH carbon. This is a dramatic deviation from the •OH radical attack on phenylalanine where attack probably takes place on the α-carbon. Tryptophan is only about 50% mineralized after 8 h of irradiation.

The two graphs on the left in Fig. 6 summarize the evolution of ammonium and nitrate ions in the photocatalyzed conversion of phenylalanine (from Fig. 5(b)) and aspartic acid as stand-alone components in the aqueous titania dis-

Table 3
Mass balance and yields of NH_4^+ and NO_3^- ions and CO_2 in the photooxidative mineralization of various amino acids and related compounds in oxygen-saturated aqueous titania suspensions

No.	Compound	Percentage yields after 8 h irradiation		
		NH_4^+	NO_3^-	CO_2
Amino acids				
1	L-α-Alanine	96	~2	100
2	β-Alanine	87	7.3	81
3	L-Valine	77	10	69
4	L-Leucine	73	18	100
5	L-iso-Leucine	67	18	86
6	L-Serine	76	10	100
7	L-Threonine	71	23	76
8	L-Aspartic Acid	92	9.6	61
9	L-Glutamic Acid	93	11	78
10	L-Glutamine	78	10	62
11	L-Cysteine	90	8.4	–
12	L-methionine	92	11	76
13	L-Phenylalanine	77	10	62
14	L-Tryptophan	68	15	49
15	L-Histidine	48	10	91
16	L-Proline	76	21	–
17	L-Arginine	25 (41) [a]	8.5 (19) [a]	57
Miscellaneous related compounds				
	Aspartame	52	5.5	–
	C_{12}-L-Glutamate	81	13	–
	C_{12}-β-Alanine	61	8	–

[a] After 50 h irradiation.

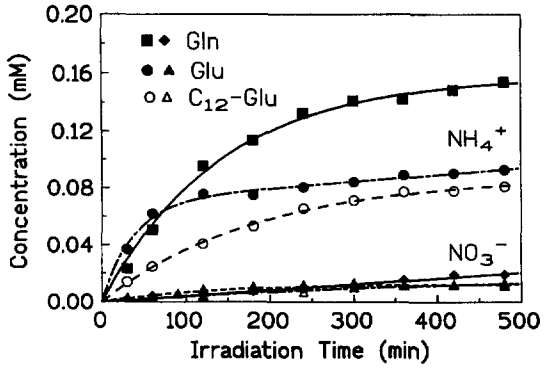

Fig. 3. Plots showing the temporal evolution of ammonia and nitrate ions during the photodegradation of glutamic acid, glutamine, and C_{12}-glutamic acid (for conditions, see experimental section).

persions. The graph on the right shows the evolution of NH_4^+ and NO_3^- ions when Phe and Asp are simultaneously present in the aqueous dispersion. It is reproduced here to illustrate the effect on the evolution of these two ions from the methyl ester product that is formed from the reaction between Phe and Asp (aspartame; see Table 1 for structure). The NH_4^+/NO_3^- ratio for Phe and Asp are, respectively, 5.0 and 9.6; for aspartic acid, conversion of the nitrogen is quantitative and it is nearly so for phenylalanine after an 8 h irradiation period (77% NH_4^+ and 10% NO_3^- for Phe; and 92% NH_4^+ and 9.6% NO_3^- for Asp; see Table 3). When the combined Phe and Asp are photoconverted, the yields of ammonium and nitrate ions are 82% and 13% (ratio: 6.3),

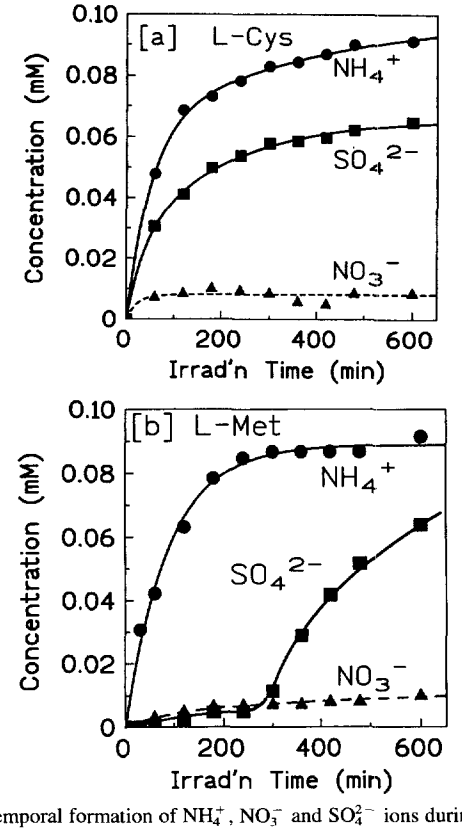

Fig. 4. Temporal formation of NH_4^+, NO_3^- and SO_4^{2-} ions during the photodegradation of (a) L-cysteine, and (b) L-methionine.

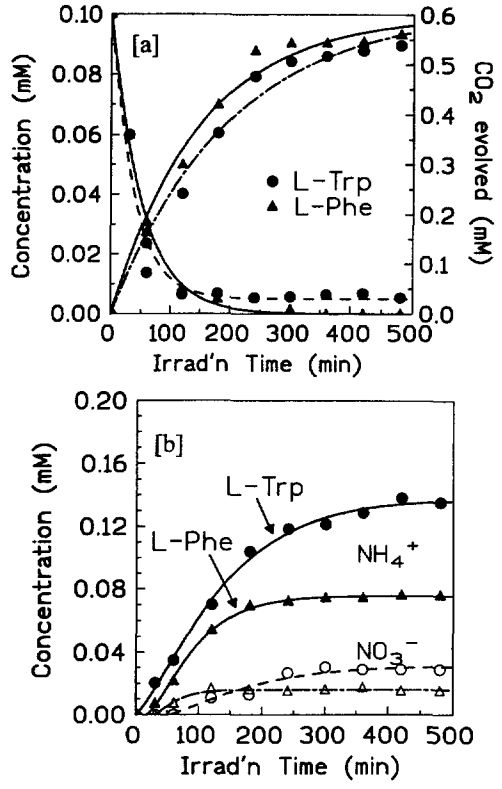

Fig. 5. (a) Disappearance of the aromatic moiety in L-tryptophan and L-phenylalanine, and evolution of carbon dioxide. (b) Formation of NH_4^+ and NO_3^- ions for the photodegradation of L-phenylalanine and L-tryptophan.

less than expected. For aspartame, the yield of NH_4^+ and NO_3^- ions has decreased significantly to 52% and 5.5%, respectively, and their formation is two-fold slower (Table 2) than for either Phe or Asp alone; the NH_4^+/NO_3^- ratio in aspartame is 9.8 nearly identical to that for aspartic acid. We infer that •OH radical attack for H-atom abstraction takes place initially on the α-carbon (***–CH–***) of the aspartic acid moiety in aspartame, since the amino function in phenylalanine is protected by formation of the amide function: **–OOCCH$_2$*CH*(NH$_2$)CO**NH–CH(CH$_2$C$_6$H$_5$)COOCH$_3$.

3.2. Proposed mechanism of photodegradation

Some of the steps in the photodegradation mechanism of amino acids are illustrated in Scheme 1. The Scheme is divided into two parts. In part (a) we examine the events that pertain to the TiO_2 photocatalyst following illumination with UV-A and UV-B radiation (see also Fig. 1; $E_{bg} = 3.2$ eV; wavelengths < 387 nm). The second part (b) looks at some of the steps in the mechanism of photooxidative and/or -reductive processes on one of the amino acids, herein chosen to be α-Ala, to examine how the mineralization products NH_3, NO_3^- and CO_2 may be formed. It is relevant to note that in so doing we do not preclude other competitive reactions in the sequence of steps.

Thus, upon irradiation of the photocatalyst and subsequent to charge formation and separation, migration of the charge carriers (conduction band electrons, e^-, and valence band

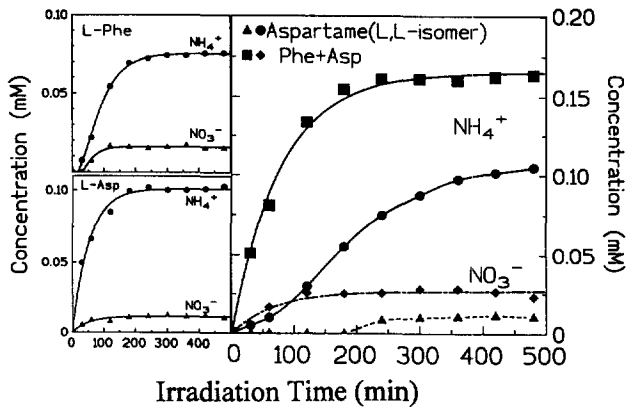

Fig. 6. Formation of NH_4^+ and NO_3^- ions during the photodegradation of L-phenylalinine, L-aspartic acid and aspartame.

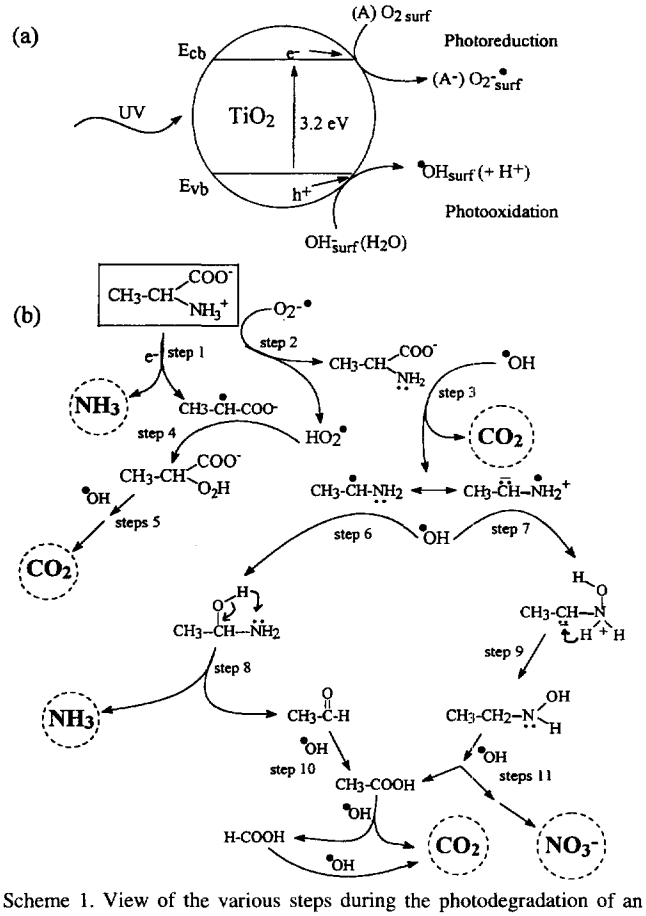

Scheme 1. View of the various steps during the photodegradation of an amino acid catalyzed by irradiated titania nanoparticulates.

holes, h^+) to the photocatalyst particle surface takes place in competition with other trapping and recombination events in the bulk of the particle. At the surface, these charge carriers are trapped and are poised to carry out redox reactions with suitable electron acceptors and donors in competition with radiative and nonradiative recombination that waste photon energy; this will influence the overall redox process efficiencies. Greater details of these events may be found elsewhere [19]. It suffices to note that at the surface the hole can oxidize the OH^- groups (and H_2O) to produce •OH radicals (and

H^+). On the reductive side, adsorbed dioxygen molecules (aerated or oxygen-saturated conditions) accept electrons and are reduced to superoxide radical anions O_2^-• which combine with H^+ to give HO_2• radicals. It is the surface-trapped electrons and the surface-bound •OH (and less so HO_2•) radicals that will induce the mineralization of the various amino acids and the DNA/RNA bases [20].

Electron attachment to the zwitterionic form of α-Ala (Eq. (1); step 1 in Scheme 1(b)) leads to deamination to give NH_3 and an α-carboxyalkyl radical [14] which upon reaction (step 4) with HO_2•, formed in step 2, produces a peroxide species (Fig. 2(c)) that ultimately undergoes further oxidation to yield CO_2 through step 5. In step 2, the superoxide radical anion is protonated by the $-NH_3^+$ function to give the unprotonated form of α-Ala. The latter is attacked by another •OH radical at the free electron pair of $-NH_2$ (step 3) to form an •OH adduct that may fragment via a process analogous to the Grob-type fragmentation reaction [9,21] and yield a N-centered radical and its resonance form CH_3–C•H–NH_2; that is, the adduct dissociates into the N-centered radical, subsequently followed by spontaneous evolution of CO_2. Reaction of •OH with CH_3–C•H–NH_2 in step 6 yields an α-OH substituted amine which breaks up to produce NH_3 and acetaldehyde (step 8), the latter being readily oxidized to acetic acid (step 10). The N-centered radical species also reacts with •OH in step 7 to give a protonated hydroxylamine intermediate, which following proton transfer yields ethyl hydroxylamine, CH_3–CH_2–NHOH (step 9). Additional attachment of •OH on this hydroxylamine at the nitrogen electron pair (or via H-atom abstraction) ultimately affords NO_3^- ions (via nitrite ions) and acetic acid. This acid can subsequently undergo oxidation via a photo-Kolbe type process (oxidation via electron transfer and decarboxylation) to generate carbon dioxide and formic acid, which also generates carbon dioxide via a similar process.

An additional pathway, not shown in Scheme 1 but probably no less important in zwitterionic forms of amino acids [14] except in the unprotonated forms [9], may implicate H-atom abstraction by •OH radicals at the α-carbon of alanine. Clearly, however, an important step is electron attachment to the zwitterion which causes deamination with formation of the α-carboxyalkyl radical [14]. For amino acids having longer alkyl chains and/or additional groups on the **$-CH(NH_3^+)COO^-$** moiety (Table 1), reactions will be governed by various factors such as the inductive effects of the amino and carboxyl groups.

By analogy with our earlier work [7e] on the photocatalyzed degradation of succinimide and N-hydroxysuccinimide, in which $[NH_3] \gg [NO_3^-]$ and $[NO_3^-] > [NH_3]$, respectively, we speculate that •OH addition to the heteroring leads to formation of hydroxylamine-type species (steps 3 and 7 in Scheme 1(b)) to give NO_3^- ions and to H-atom abstraction to produce carbon-centered radicals (steps 3, 6 and 8) to ultimately produce NH_3 as some of the initial steps in an otherwise complex sequence of events.

4. Conclusions

Amino acids are photodegraded when exposed to UV-A and UV-B radiation in the presence of aqueous TiO_2 dispersions. Formation of NH_3 implicates both TiO_2 surface electrons and surface •OH radicals. The ratio NH_3/NO_3^- spans the range 3–12 and is dependent upon the structural nature of the amino acids. In all amino acids examined, this ratio favors NH_3 formation. By contrast, formation of NO_3^- ions appears to predominate in the photodegradation of DNA and RNA bases [20].

Acknowledgements

The work in Tokyo was generously supported by a Grant-in-Aid for Scientific Research from the Japanese Ministry of Education (No. 06640757) and from the Cosmetology Research Foundation. The work in Montreal is supported by the Natural Sciences and Engineering Research Council of Canada. The authors are also grateful to the Ajinomoto Co. Ltd. for the gift of amino acids and Degussa AG for the gift of the titania catalyst.

References

[1] C. Maillard, C. Guillard, P. Pichat, M.A. Fox, New J. Chem. 16 (1992) 821.
[2] C. Maillard, C. Guillard, H. Courbon, P. Pichat, Environ. Sci. Technol. 28 (1994) 2176.
[3] (a) E. Pelizzetti, C. Minero, P. Piccinini, M. Vincenti, Coord. Chem. Rev. 125 (1993) 183; (b) P.L. Yue, D. Allen, in: D.F. Ollis, H. Al-Ekabi (Eds.), Photocatalytic Purification and Treatment of Water and Air, Elsevier, Amsterdam, 1993, p. 607; (c) E. Pelizzetti, C. Minero, V. Carlin, M. Vincenti, M. Dolci, Chemosphere 24 (1992) 891; (d) E. Pelizzetti, C. Minero, V. Maurino, Adv. Colloid Interface Sci. 32 (1990) 271; (e) E. Pelizzetti, C. Minero, E. Pramauro, M. Barbeni, V. Maurino, M. Tosato, Chim. Ind. (Milano) 69 (1987) 88; (f) E. Pelizzetti, V. Maurino, C. Minero, O. Zerbinati, E. Borgarello, Chemosphere 18 (1989) 1437.
[4] (a) C.K.-C. Low, S.R. McEvoy, R. Matthews, Environ. Sci. Technol. 25 (1991) 460; (b) G.K.-C. Low, S.R. McEvoy, R. Matthews, Chemosphere 19 (1989) 1611.
[5] J.C. D'Oliveira, C. Gillard, C. Maillard, P. Pichat, J. Environ. Sci. Health, A28 (1993) 941.
[6] K. Waki, L. Wang, K. Nohara, H. Hidaka, J. Mol. Catal. 95 (1995) 53.
[7] (a) H. Hidaka, J. Zhao, E. Pelizzetti, N. Serpone, J. Phys. Chem. 96 (1992) 2226; (b) H. Hidaka, J. Zhao, Colloids Surf. 67 (1995) 145; (c) H. Hidaka, K. Nohara, J. Zhao, K. Takashima, E. Pelizzetti, N. Serpone, New J. Chem. 18 (1994) 541; (d) H. Hidaka, K. Nohara, J. Zhao, E. Pelizzetti, N. Serpone, J. Photochem. Photobiol. A: Chem. 91 (1995) 145; (e) K. Nohara, H. Hidaka, E. Pelizzetti, N. Serpone, Catal. Lett. 36 (1996) 115; (f) K. Nohara, H. Hidaka, E. Pelizzetti, N. Serpone, J. Photochem. Photobiol. A: Chem., 102 (1997) 279.
[8] A. Avranas, I. Poulios, C. Kypri, D. Jannakoudakis, G. Kyriakou, Appl. Catal. B2 (1993) 289.
[9] J. Momig, R. Chapman, K. Asmus, J. Phys. Chem. 89 (1985) 3139.

[10] A. Fujishima, R. Cai, K. Hashimoto, H. Sakai, Y. Kubota, in: D.F. Ollis and H. Al-Ekabi (Eds.), Photocatalytic Purification and Treatment of Water and Air, Elsevier, Amsterdam, 1993, p. 193.
[11] J. Monig, M. Gobl, K.-D. Asmus, J. Chem. Soc., Perkin Trans. II (1985) 647.
[12] K.-D. Asmus, M. Gobl, K.-O. Hiller, S. Mahling, J. Monig, J. Chem. Soc., Perkin Trans. II (1985) 641.
[13] N. Konigsberg, G. Stevenson, J.M. Luck, J. Biol. Chem. 235 (1960) 1341.
[14] P. Neta, M. Simic, E. Hayon, J. Phys. Chem. 74 (1970) 1214.
[15] K.-O. Hiller, B. Masloch, M. Gobl, K.-D. Asmus, J. Am. Chem. Soc. 103 (1981) 2734.
[16] V.C. Hand, M.P. Snyder, D.W. Margerum, J. Am. Chem. Soc. 105 (1983) 4022.
[17] S. Hara, Y. Kuroda, S. Nakagawa, Y. Totani, J. Jpn. Oil Chem. Soc. 43 (1994) 18.
[18] F.A. Carey, Organic Chemistry, 2nd ed., McGraw-Hill, New York, 1992.
[19] N. Serpone, D. Lawless, R. Khairutdinov, E. Pelizzetti, J. Phys. Chem. 99 (1995) 16655.
[20] H. Hidaka, S. Horikoshi, N. Serpone, J.B. Knowland, Photochem. Photobiol., to be submitted.
[21] C.A. Grob, Angew. Chem., Int. Ed. Engl. 8 (1969) 535.